DOI: 10.1111/nyas.14816

ORIGINAL ARTICLE

ANNALS OF THE NEW YORK ACADEMY OF SCIENCES

MicroRNA-21-5p functions via RECK/MMP9 as a proalgesic regulator of the blood nerve barrier in nerve injury

Ann Kristin Reinhold[1] | Susanne M. Krug[2] | Ellaine Salvador[1,3] | Reine S. Sauer[1] | Franziska Karl-Schöller[4] | Marzia Malcangio[5] | Claudia Sommer[4] | Heike L. Rittner[1]

[1]Department of Anesthesiology, Intensive Care, Emergency and Pain Medicine, University Hospital Würzburg, Center for Interdisciplinary Pain Medicine, Würzburg, Germany

[2]Institute of Clinical Physiology/Nutritional Medicine, Charité - Universitätsmedizin Berlin, Berlin, Germany

[3]Section Experimental Neurosurgery, Department of Neurosurgery, University Hospital Würzburg, Würzburg, Germany

[4]Department of Neurology, University Hospital Würzburg, Würzburg, Germany

[5]Wolfson Centre for Age-Related Diseases, Institute of Psychiatry, Psychology and Neuroscience, King's College London, London, UK

Correspondence
Heike L. Rittner, Department of Anesthesiology, Intensive Care, Emergency and Pain Medicine, University Hospital Würzburg, Center for Interdisciplinary Pain Medicine, Oberdürrbacher Str. 6, 97080 Würzburg, Germany.
Email: Rittner_h@ukw.de

Funding information
FP7 Health, Grant/Award Number: ncRNAPain 602133; Interdisziplinäres Zentrum für Klinische Forschung, Universitätsklinikum Würzburg, Grant/Award Number: Z-2/61; Deutsche Forschungsgemeinschaft, Grant/Award Number: KFO 5001

Abstract

Both nerve injury and complex regional pain syndrome (CRPS) can result in chronic pain. In traumatic neuropathy, the blood nerve barrier (BNB) shielding the nerve is impaired—partly due to dysregulated microRNAs (miRNAs). Upregulation of microRNA-21-5p (miR-21) has previously been documented in neuropathic pain, predominantly due to its proinflammatory features. However, little is known about other functions. Here, we characterized miR-21 in neuropathic pain and its impact on the BNB in a human-murine back translational approach. MiR-21 expression was elevated in plasma of patients with CRPS as well as in nerves of mice after transient and persistent nerve injury. Mice presented with BNB leakage, as well as loss of claudin-1 in both injured and spared nerves. Moreover, the putative miR-21 target RECK was decreased and downstream *Mmp9* upregulated, as was *Tgfb*. *In vitro* experiments in human epithelial cells confirmed a downregulation of *CLDN1* by miR-21 mimics via inhibition of the *RECK/MMP9* pathway but not *TGFB*. Perineurial miR-21 mimic application in mice elicited mechanical hypersensitivity, while local inhibition of miR-21 after nerve injury reversed it. In summary, the data support a novel role for miR-21, independent of prior inflammation, in elicitation of pain and impairment of the BNB via RECK/MMP9.

KEYWORDS
blood nerve barrier, claudin-1, CRPS, microRNA, MMP9, neuropathic pain, RECK

INTRODUCTION

Chronic pain is a frequent medical condition, placing a heavy burden on both patient and the health system alike. While its manifold pathophysiology has been increasingly understood in recent years, current treatment options prove still insufficient. This is particularly true for complex regional pain syndrome (CRPS), characterized by disproportionate ongoing pain after trauma, for example, fracture. Symptoms include hypersensitivity and allodynia, edema and sweating, motor and trophic changes, as well as changes in skin color and temperature.[1] One aspect of peripheral neuropathic pain that has recently gained attention is the impairment of the blood nerve barrier (BNB). The

BNB protects the nerve from noxious stimuli and consists mainly of the perineurium surrounding the peripheral nerve fascicle and the endothelium of endoneurial blood vessels.[2] The BNB is formed by tight junctions with their proteins, including members of the claudin family, such as claudin-1, the main component of the perineurial barrier.[4] Previously, we demonstrated that traumatic neuropathy in mice such as chronic constriction injury (CCI; a ligation of the sciatic nerve) leads to an increased BNB permeability, accompanied by quantitative and qualitative changes in key tight junction proteins.[3]

MicroRNAs (miRNAs) are single-stranded short noncoding RNAs that, within the last decade, have gained attention as switches in various pathologies, including neurological diseases. Moreover, miRNA signatures change in several pain entities, including in CRPS.[5–7] MiR-21 regulates both neuropathic pain and barrier disruption. In peripheral neuropathy models, for example, spared nerve injury (SNI), miR-21-5p is upregulated in dorsal root ganglion (DRG) neurons.[8] In painful polyneuropathy, miR-21 levels rise both locally, in sural nerve biopsies, and systemically, in white blood cells.[7] While proinflammatory miR-21 interactions in the context of pain are well-characterized,[9,10] little is known about the effects independent of inflammation. Studies suggest a destabilizing effect of circulating miR-21 on the blood brain[11] and intestinal barriers.[12] However, few studies have looked at miR-21 in the peripheral nerve,[10,13] and none have considered the BNB.

Confirmed targets of miR-21-5p are matrix metalloproteinase (MMP) suppressors phosphatase and tensine homolog (PTEN) and reversion inducing cysteine-rich protein with Kazal motifs (RECK).[14] MMPs, such as MMP9, contribute to both the initiation of neuropathic pain and barrier disruption via regulating claudins.[14,15] Moreover, miR-21 positively regulates transforming growth factor beta (TGF-β), an anti-inflammatory cytokine also involved in barrier impairment.[16,17]

As miR-21 targets include barrier-related pathways, and barrier impairment contributes significantly to neuropathic pain,[2] in our study here, we evaluated the function of miR-21 on the BNB. Two possible mechanisms were investigated: the RECK–MMP9 pathway and a regulation via TGF-β. We examined miR-21 regulation in CRPS patients and in mouse models of persistent (SNI) and transient (CCI) neuropathic pain. To further characterize miR-21–dependent effects, we studied the impact of miR-21 mimic application *in vivo* and *in vitro*, in a human cellular barrier model.

MATERIALS AND METHODS

Patients

Patients were a subgroup from Würzburg of the cohort for the EU 7FP ncRNAPain project following the ncRNAPain study protocol (German registry for clinical studies, registration number DRKS00008964). They gave written informed consent and underwent clinical and neurological examination, as well as blood sampling. Patients who did not develop CRPS after trauma in the past year (fracture controls, FC) undergoing the same examinations served as controls. By definition, CRPS patients fulfilled the diagnostic Budapest criteria, whereas FC did not. Among parameters collected was the CRPS severity score (CSS), which includes symptoms reported by the patients and signs observed by the examiner and the Neuropathic Pain Symptom Inventory (NPSI). Details on the entire cohort have already been described.[18]

Plasma preparation

Blood samples (Sarstedt S-monovette EDTA, 9 ml, Sarstedt, Nürnbrecht, Germany) were drawn from patients in the morning, after overnight fasting. After centrifugation at 1300*g* for 10 min (room temperature), the supernatant was aliquoted and stored at −80°C.

Animals

Young adult male C57BL/6 mice (Janvier Labs, Le Genest-Saint-Isle, France) were housed in groups of four in sawdust cages with a 12 h light/dark cycle and water and food provided ad libitum. Littermates were randomized: Two animals of each cage were allocated to the study group, the others to the control group. Environmental enrichment was provided. Animals were checked daily for signs of stress or illness. During experiments, animal welfare was assessed via daily score sheets. A biostatistician calculated sample sizes beforehand, based on the literature research and previous experience. Animal experiments were approved by the regional authorities (Regierungsbehörde Unterfranken, protocol 44/14).

Surgery

For surgical procedures and injections, mice were anaesthetized with isoflurane 1.5 Vol% (Baxter, Deerfield, IL, USA). In CCI, the skin of the left thigh was incised, and the sciatic nerve was located and exposed; three friction-knotted loose ligations were tied around the sciatic nerve at mid-thigh level nerve using 6-0 silk threads (Permahand Silk, Ethicon, Rariton, NJ, USA) and the wound was closed with skin sutures[3] (adapted from[19]). Sham surgery consisted of anesthesia and exposure of the nerve without nerve ligation followed by skin suture. In SNI, skin and muscle of the left thigh were incised to expose the sciatic nerve and its three terminal branches; the common peroneal and tibial nerves were tightly ligated using a 6-0 silk thread and the distal nerve stump was removed, while the sural nerve was left intact.[20] In sham-injured mice, the sciatic nerve was exposed but not ligated or excised.

Perineural injections

Perineurial injections were performed using a 1 ml insulin syringe with a 26G needle. Before the first injection, fur was shaved off in a small area at the left thigh. After disinfection, the needle was carefully inserted at the dorsolateral thigh, until a gentle twitch of the paw

indicated proximity to the sciatic nerve. At this position, 50 μl of mimic or antagomiR was injected. After removal of the needle, the site of injection was checked for swelling or bleeding and again disinfected. Animals were sacrificed via exsanguination under deep isoflurane anesthesia.

Drug application

Mimic

One nanomole of mimic in 50 μl PBS (pH 7.4) was slowly injected. Mimics (mmu-mir-21-5p and cel-mir-67 as control) were custom-made with 5′ fluorescein label and 3′ cholesterol (Dharmacon, Lafayette, CO, USA). Injections were performed daily, for up to 7 consecutive days.

AntagomiR

Custom-made LNA-based mmu-miR-21-5p *in vivo* antagomiR or scrambled control (Exiqon, Vedbæk, Denmark) was incubated in i-Fect™ transfection reagent (Biobyrt, Cambridge, UK) 1:5 for 5 min. Five picomoles in 50 μl PBS were injected daily for 5 days, starting either directly after CCI or at 7 days after surgery.

Sequences

MiR-21-5p-antagomiR: /5FAM/T*C*A*G*T*C*T*G*A*T*A*A*G*C*T; scrambled oligomer: /5FAM/T*C*A*G*T*A*T*T*A*G*C*A*G*C*T with /5FAM/ indicating FAM labeling of the 5′ end and * indicating a 6 phosphorothioate bond, a modification needed for *in vivo* stability.

Behavioral analysis

In CCI, paw withdrawal threshold (PWT) was examined prior to and daily after surgery. For perineurial drug injection, PWT was tested prior to the first dosage and 6 h after each injection. PWT was determined with von Frey filaments (Ugo Basile, Gemonio, Italy), increasing and decreasing stimulus intensity, using Dixon's up and down method.[21]

qPCR

Nerve tissue samples were homogenized in QIAzol Lysis Reagent containing sterile metal beads, using the Tissue Lyzer (Qiagen, Hilden, Germany) for 4 min at 20/sec. RNA was isolated from the homogenate with the Qiagen miRNeasy kit (Qiagen), following manufacturer's instructions. For plasma samples, the miRNeasy Serum/Plasma kit (Qiagen) was used, according to the manufacturer's protocol. RNA concentration and purity was measured with a Nanodrop ND 2000 spectrometer (Thermo Fischer Scientific, Waltham, MA, USA) at 260/280 nm. For miRNA analysis, we used the TaqMan™ MicroRNA Reverse Transcription Kit (input 5 ng total RNA per sample) and TaqMan™ Universal PCR Master Mix (Applied Biosystems, Waltham, MA, USA) following manufacturer's instructions. SnU6 served as reference gene. The following TaqMan™ assays were used: hsa-miR-21, mmu-miR-21: 00397, U6 snRNA: 001973. For mRNA experiments, 1 μg total RNA per sample was reverse-transcribed to cDNA using the high-capacity cDNA kit (with random primer and RNAse inhibitor, Applied Biosystems) according to the manufacturer's protocol. qPCR analysis was performed using the SYBR®Green technique. Master mix was prepared for 10 μl/well: 50 ng cDNA in 1 μl H_2O, 5 μl PowerUp™ SYBR®Green Master Mix (Thermo Fischer Scientific), 250 μM of each forward and reverse primer, and 3 μl H_2O. *Gapdh* served as reference gene. The custom following primers were used, based on PrimerBlast-guided design for *Mus musculus* (PrimerBlast, NIH): *Cldn1*: forward CTGTGGATGTCCTGCGTTTC, reverse TTACCATCAAGGCTCGGGTT; *Mmp9*: forward AGACGACATAGACGGCATCC, reverse CTGTGGTTCAGTTGTGGTGG; *Reck*: forward CGGGTGCTGTATGCTGTAATC, reverse GCAACAGATGTTTCAGTCGGG; *Tgfb*: forward ATGCTAAAGAGGTCACCCGC, reverse TGCTTCCCGAATGTCTGACG; *Gapdh*: forward AGTCTACTGGCGTCTTCAC, reverse TCATATTTCTCGTGGTTCAC; (MWG Eurofins, Ebersberg, Germany). qPCR analysis was carried out by a StepOnePlus™ Real-Time PCR System (Thermo Fischer Scientific) using the following settings: 2 min at 50°C, 2 min at 95°C, 40 cycles with 3 s at 95°C and 30 s at 60°C. For all experiments, samples were analyzed as triplicates. Relative mRNA expression was calculated using the dCt method.

In vitro analysis

For *in vitro* analysis of mRNA changes due to miR-21, the epithelial cell line HT-29/B6,[22] which forms well-differentiated barriers containing high levels of claudin-1, was chosen to allow comparison to former studies. Cells were transfected with either 2 μg hsa-miR-21 mimic (hsa-miR21-5p; 473093_001; Applied Biosystems/Thermo Fisher Scientific) or Cel (cel-miR39-3p; 479902_001; Applied Biosystems/Thermo Fisher Scientific) using Lipofectamin 2000 (Thermo Fisher Scientific) according to the manufacturer's instructions. mRNA was harvested 48 h after transfection parallel to an untransfected control using the NEBNext Poly(A)mRNA magnetic isolation module (New England Biolabs GmbH, Frankfurt, Germany) followed by reverse transcription of 3 μg RNA (in 50 μl) into cDNA using MultiScribe Reverse Transcriptase (Thermo Fisher Scientific). Real-time qPCR reactions were performed using 1 μl of cDNA template, 1 μl of the probe of interest, 1 μl of the reference probe, 10 μl of RT-qPCR Master Mix (Applied Biosystems/Thermo Fisher Scientific), and nuclease-free water to a final volume of 20 μl. The following Taqman probes, designed for the human genome, were used (all from Applied Biosystems/Thermo Fisher Scientific): Cldn1 (Hs00221623_m1), TGFB (Hs00234253_m1),

MMP9 (Hs00957562_m1), RECK (Hs01019185_m1), and GAPDH (Hs02786624_g1) as reference. Comparative CT reactions were performed in duplicates using a 7500 Fast Real-Time PCR System (Applied Biosystems). Calculations for gene expression changes were performed using the $2^{-\Delta\Delta CT}$ method. For western blot analysis, proteins were prepared from the protein-containing phenol-fraction of RNA preparations, precipitating them with acetone. Purification was done by several washing steps of the protein pellets with 0.3 M guanidine hydrochloride in 95% ethanol + 2.5% glycerol (v:v). Finally, after washing with ethanol containing 2.5% glycerol (v:v), proteins were dried after pelleting and resolved in total lysis buffer (10 mM Tric-Cl pH 7.5, 150 mM NaCl, 0.5% Triton X-100, 0.1% SDS, protease inhibitors). Proteins were separated by sodium dodecyl sulphate-polyacrylamide gel electrophoresis and immunoblotted on PVDF membranes (Perkin Elmer, Rodgau, Germany). For immunodetection, membranes were incubated in blocking solution (1% polyvinylpyrrolidone-40, 0.5% Tween) and incubated over night with primary antibodies (rabbit anti-Claudin-1 [Invitrogen, Cat. 519000], goat anti-MMP9 [R&D, Cat. AF911], mouse anti-TGF-beta [R&D, Cat. MAB1835], and mouse anti-beta-Actin [Sigma-Aldrich, CAT. A5441]). After washing steps and incubation with peroxidase-coupled secondary antibodies, proteins were detected using SuperSignal West Pico PLUS (Thermo Fisher Scientific) and a Fusion FX7 (Vilber Lourmat). Densitometric analysis was done using AIDA (Elysia).

Permeability testing

To measure the perineurial permeability for large molecules, the excised sciatic nerve was immediately fixed in 1% PFA for 1 h and immersed in 2 ml of Evan's Blue Albumin (EBA, 68 kDa, 5% bovine albumin labeled with 1% Evans Blue; Sigma Chemicals, St. Louis, MO, USA) for 1 hour. After embedding in TissueTek O.C.T. Compound (Sakura, Alphen aan den Rijn, Netherlands), 10 μm sections were obtained via cryostat (Leica Biosystems, CM3050 S Cryostat, Nussloch, Germany) and analyzed by microscopy (Biorevo BZ-9000-E, Keyence, Osaka, Japan).

Immunohistochemistry

To assess the organization of tight junctions in the perineurium, especially claudin-1 distribution, after nerve injury and mimics injection, we performed immunohistochemistry of the sciatic nerve. The sciatic nerve was harvested, snap-frozen in liquid nitrogen, embedded in TissueTek O.C.T. Compound (Sakura), the entire vial then snap-frozen and stored at −20°C. Using a cryostat, 10 μm sections were cut. For immunofluorescence labeling, slices were fixed in ethanol (Sigma Aldrich), permeabilized with 0.5% Triton X-100 (Sigma Aldrich) in PBS, and blocked with 10% donkey serum in PBS. Next, the sections were incubated with primary antibodies at 4°C overnight: rabbit anti-claudin-1 (1:100, 51–9000, Thermo Fischer Scientific) and goat anti-ZO-1 (1:150, orb153344, Biorbyt). After washing in PBS, nerve samples were incubated with secondary antibodies in PBS: For claudin-1, Alexa Fluor 555 donkey anti-rabbit LgG (1:1000, A31572), for ZO-1, Alexa Fluor 488 donkey anti-goat IgG (1:1000, A11055, both Life Technologies, Eugene, OR, USA). After washing, the sections were mounted with VectaShield Antifade Mounting Medium (Vector Laboratories, Burlingame, CA, USA). Stainings were visualized by immunofluorescence microscopy (Biorevo BZ-9000-E, Keyence). Z-stacks (1 μm) were saved in RGB 8-bit TIFF pictures.

TABLE 1 Demographic and clinical characteristics of the patient cohort

	CRPS	FC
n	30	20
Age (years)	50.2 ± 10.3	40.4 ± 12.3
Female/male	24/6	9/11
Mean pain last week (NRS)	5.4 ± 1.9	2.3 ± 1.8
CSS	12 ± 2.5	1 ± 0.9
Upper/lower extremity	27/1	20
CRPS I/CRPS II	22/8	n.a.
Warm/cold CRPS	22/7	n.a.
NPSI	0.40 ± 0.23	n.a.
Cause of trauma (fracture/other)	16/14	17/3
Time since diagnosis (years)	2.2 ± 2.7	0.6 ± 0.45
Duration of pain due to disease (years)	2.4 ± 2.6	0.6 ± 0.4

Note: Causes of trauma other than fracture include surgery and rupture of ligaments and tendons. Values are given as mean ± SD where applicable.
Abbreviations: CSS, CRPS severity score; FC, fracture control; n.a., not applicable; NPSI, neuropathic pain symptom inventory; NRS, numeric rating scale.

Statistical analysis

Statistical analysis was performed and graphs were generated using Prism GraphPad software (GraphPad, San Diego, CA, USA). Comparison of two groups was performed using a *t*-test or a nonparametric test; to determine if data were normally distributed we used the Shapiro–Wilk test. More than two groups were compared using ANOVA. Specific tests are indicated in the figure legends. If not stated otherwise, results are given as mean ± SEM. Results were considered significant at $p < 0.05$.

RESULTS

miR-21 is elevated in CRPS and murine nerve injury

We quantified miR-21 in plasma from CRPS patients and fracture controls, that is, patients who did not develop CRPS after trauma (Table 1). The typical CRPS patient was middle-aged, female, with a

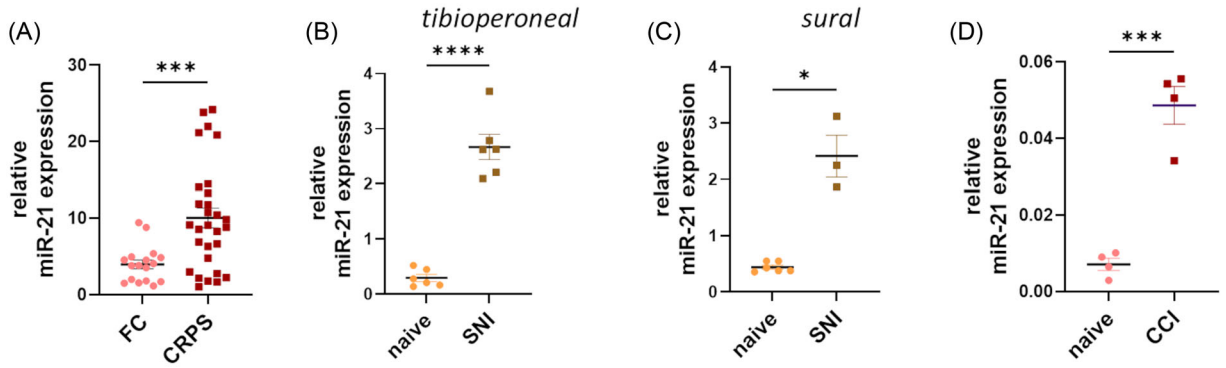

FIGURE 1 MiR-21 elevation in chronic neuropathic pain conditions in humans and mice. miR-21-5p was quantified in (A) plasma of CRPS patients ($n = 30$) and fracture controls ($n = 20$), in (B, C) SNI mice 7 days after surgery and naive controls in the common tibioperoneal nerve and the sural nerve ($n = 3–6$), and (D) in CCI mice 7 days after surgery in the sciatic nerve compared to naive controls ($n = 4$). $^{*}p < 0.05$, $^{***}p < 0.001$, $^{****}p < 0.0001$. All Welch's test. Abbreviation: FC, fracture control

warm CRPS I of the upper extremity, moderate pain, and symptoms typical of neuropathic pain (as assessed by the NPSI). In contrast, FC did not show characteristic signs and symptoms of CRPS and reported only mild pain intensity. miR-21 levels were 2.5-fold increased in CRPS patients compared with controls (Figure 1A). While miR-21 levels did correlate moderately with CRPS severity (CRPS severity score, CSS), this could not be linked to single items of the CSS. Moreover, there was no correlation with pain intensity, neuropathic pain symptom inventory, CRPS type, disease duration, or the affected extremity (Tables S1 and S2). In mice, nerves of both SNI and CCI animals expressed higher miR-21 levels than respective controls 7 days after injury (Figure 1B–D). Seven days after SNI, miR-21 expression was nine-fold upregulated in the injured common tibial and peroneal nerve and 5.5-fold in the spared, intact sural nerve (Figure 1B,C). In CCI, miR-21 expression was 6.8-fold increased (Figure 1D).

BNB is impaired in permanent/transient nerve injury, with alterations in *Mmp9*, *Reck*, and *Tgfb*

Seven days after SNI, we observed EBA fluorescence signals within the nerve after *ex vivo* nerve immersion, indicating increased perineurial permeability (Figure 2A). This was paralleled by a decrease in *Cldn1*, both in the tibio-peroneal and intact sural nerve (Figure 2B,C). Moreover, structure analysis of claudin-1 and ZO-1 immunoreactivity revealed a homogenous immunoreactivity versus a cell contact-based immunoreactivity (perineurial zig zag pattern) in both tibio-peroneal and sural nerve (Figure 2D). In addition, *Mmp9* (Figure 2E,F) and *Tgfb* (Figure 2G,H) were increased. CCI led to a decrease in *Cldn1* in the damaged nerve (Figure 3A), in line with our earlier reports of BNB impairment, for example, perineurial EBA penetration and loss of cell contact-based claudin-1 immunoreactivity.[3] In addition, *Reck* was reduced in the nerve (Figure 3B), while *Tgfb* was upregulated (Figure 3C).

Perineural injection of miR-21 mimic elicits Cldn1 downregulation and redistribution

To understand the effect of miR-21 in the intact nerve, we applied miR-21 mimic locally (Figure 4A). Daily perineural injections of miR-21 mimic decreased *Cldn1* by 72% (Figure 4B). Moreover, immunoreactivity of claudin-1 in the perineurium was redistributed intracellularly indicating organizational loss from cell–cell contacts (zig-zag pattern, Figure 4C,D).

MiR-21 mimic in human HT29/B6 cells affects *RECK*, *MMP9*, and *CLDN1* but not *TGFB*

We next investigated the pathway of miR-21 and tight junction impairment *in vitro* in the human HT29/B6 epithelial cell line, which has been used before as a barrier model for the perineurium.[15,22] Forty-eight hours after incubation with hsa-miR-21 mimic, *CLDN1* was decreased by 56% (Figure 5A). Based on our observations in the mouse models, we further explored the two putative pathways, either a targeting of RECK with consecutive rise in MMP9, or via TGFB. After incubation, *RECK* was markedly reduced (Figure 5B), while *MMP9* increased (Figure 5C). In contrast, *TGFB* did not change after miR-21 mimic incubation (Figure 5D). On a protein level, we observed differential expression only at a later time point, after 72 h. These were in line with mRNA results: CLDN1 was less expressed, while MMP9 increased (Figure 5E,F). No change was observed in TGFB (Figure 5G).

Perineural miR-21 mimic elicits mechanical hypersensitivity; miR-21 antagomiR alleviates CCI symptoms

Daily perineural injections of miR-21 mimic (Figure 4A) led to mechanical hypersensitivity in the affected limb: reduced PWT in von Frey

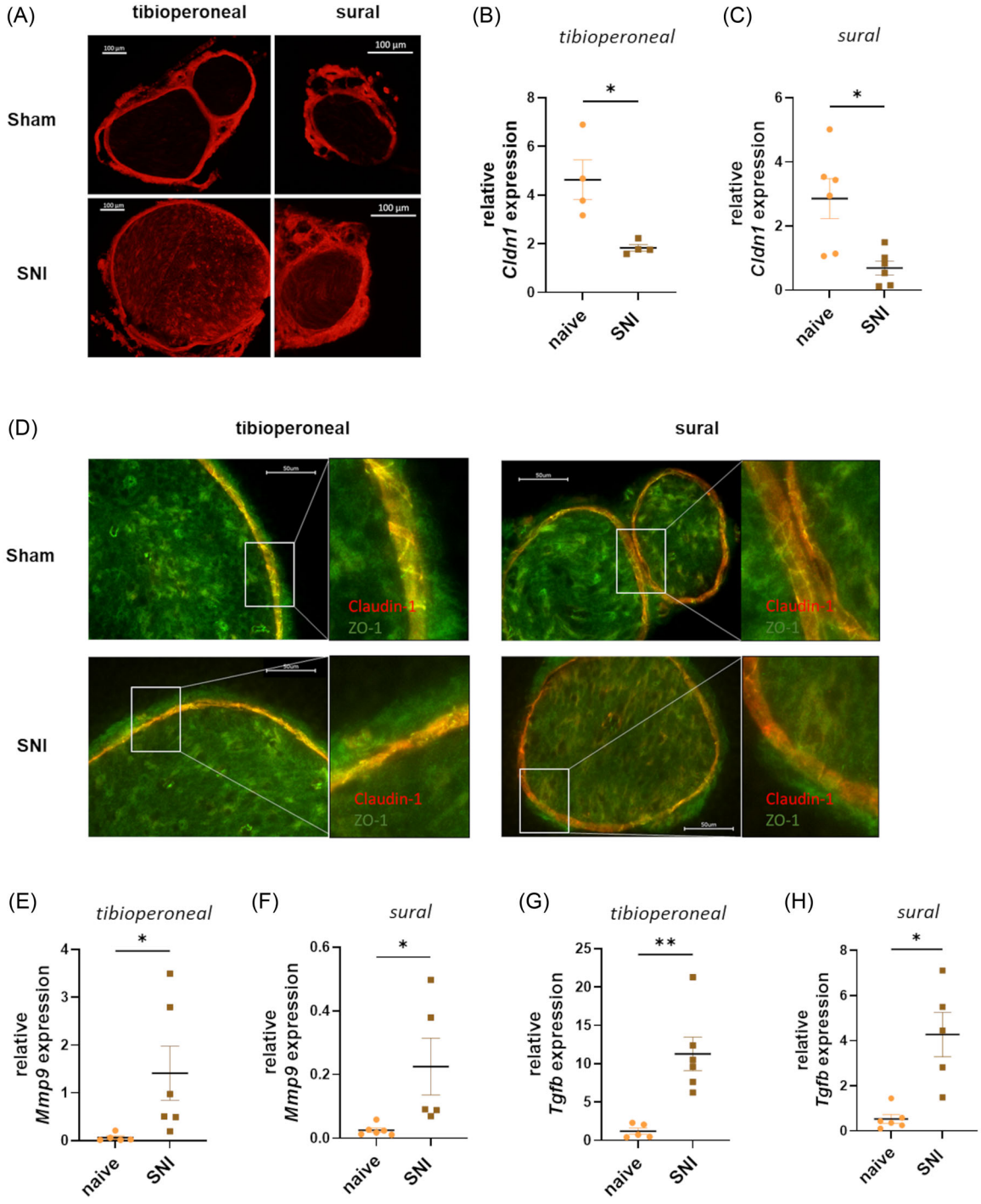

FIGURE 2 BNB opening and target gene upregulation in permanent nerve injury (SNI). Mice underwent either sham or SNI surgery. The common tibioperoneal and sural nerve were harvested on day 7. (A) Evan's Blue albumin fluorescence (68 kDa) penetration through the perineurium after surgery and *ex vivo* dye application (left: common tibioperoneal nerve, right: sural nerve, top: sham injury, bottom: SNI). Bar = 100 µm. Representative images, $n = 2$. (B, C) *Cldn1* expression compared to naive control in the common tibioperoneal and sural nerve. $n = 4–6$. (D) Immunohistochemistry after surgery. Left: common tibioperoneal nerve, right: sural nerve, top: sham injury, bottom: SNI. Claudin-1 is stained in red, ZO-1 in green, merged pictures. Bar = 50 µm. Representative images, $n = 2$ animals/group. (E, F) *Mmp9* expression in the common tibioperoneal and sural nerve after SNI compared to naive controls. $n = 5–6$. (G, H) *Tgfb* expression in the common tibioperoneal and sural nerve compared to naïve controls. $n = 5–6$. All Welch's test, $^{*}p < 0.05$, $^{**}p < 0.01$

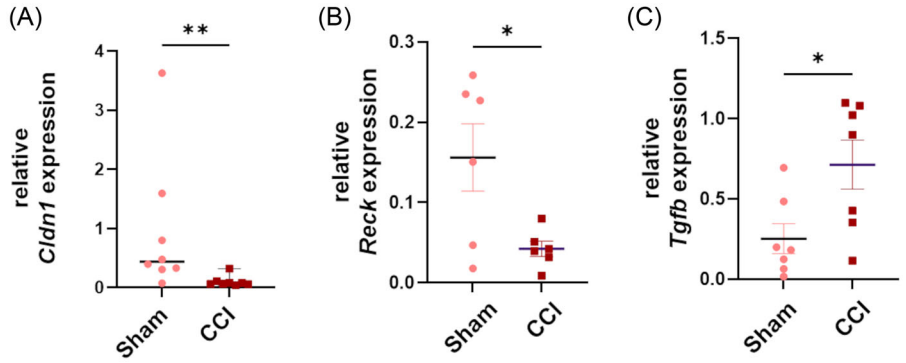

FIGURE 3 *Cldn1* and *Reck* downregulation, but *Tgfb* upregulation in transient nerve injury. Relative expression of *Cldn1* (A), *Reck* (B), and *Tgfb* (C) to *Gapdh* in the sciatic nerve 7 days after CCI compared to sham controls. (A) Mann–Whitney test, bar = median. (B, C) Welch's *t*-test, $n = 6–8$, $^*p < 0.05$

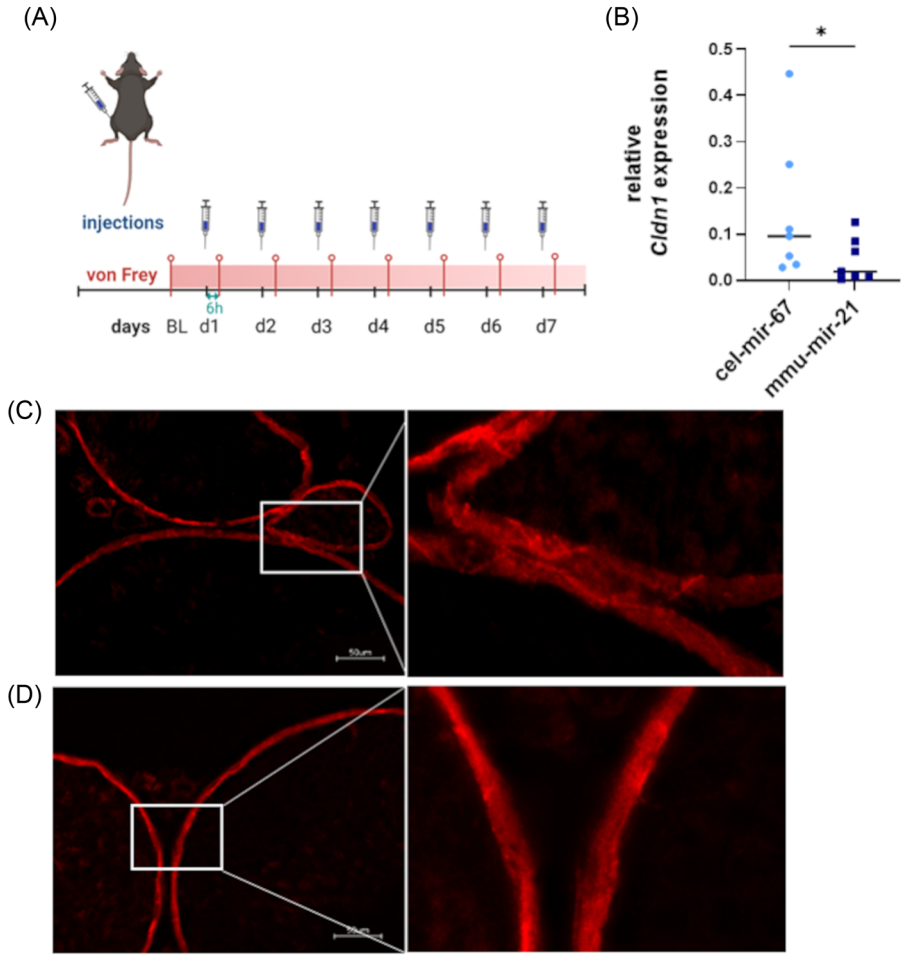

FIGURE 4 Reduced *Cldn1* and claudin-1 redistribution from cell–cell contracts in the perineurium after perineural miR-21 mimic injection. (A) Injection scheme: Daily mimic injections were followed by behavioral testing after 6 h. Control: cel-miR-67. Created with biorender®. (B) Relative *Cldn1* to *Gapdh* expression after two injections. Mann–Whitney test, $n = 7$, $^*p < 0.05$. Bar = median. (C, D) Immunostaining of the sciatic nerve for claudin-1 after two injections of cel-miR-67, C, or mmu-miR-21, D. Bar = 50 μm. Representative images, $n = 2$ animals per group. Abbreviations: BL, baseline; Von Frey, von Frey filament testing

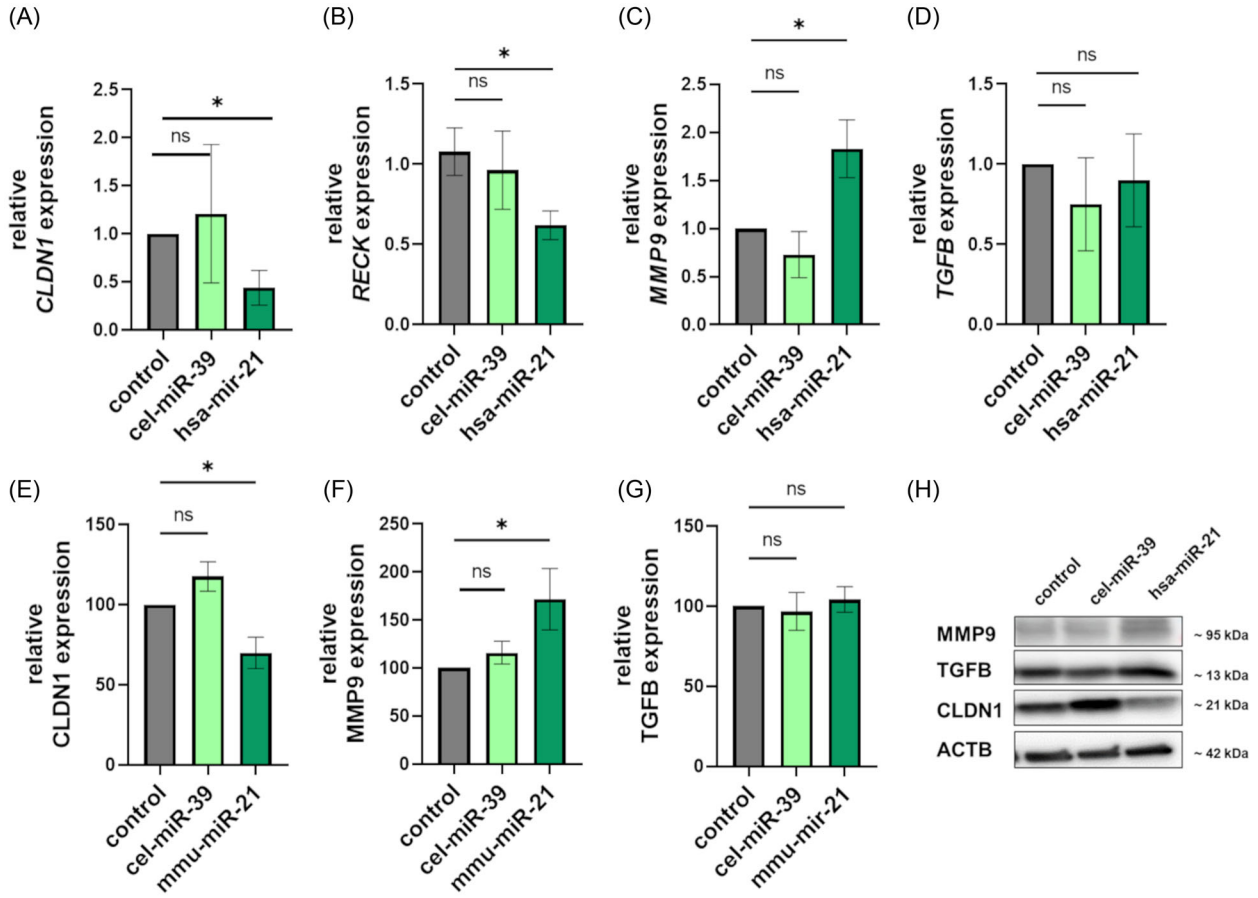

FIGURE 5 Target gene expression after miR-21 mimic incubation of HT-29/6B cells. Relative expression of *CLDN1* (A), *RECK* (B), *MMP9* (C), and *TGFB* (D) in HT-29/6B cells after 48 h of mimic incubation. (E–G) Relative protein expression of *CLDN1*, E, *MMP9*, F, and *TGFB*, G, 72 h after mimic incubation. (H) Corresponding blots. $n = 5–8$, Student's *t*-test with Bonferroni–Holm correction, $^*p < 0.05$

testing after two injections and remaining at this level for the remainder of the injections (in total 7 days) (Figure 6A). The opposite was true for miR-21 inhibition (Figure 6B): starting immediately after CCI, daily perineural injections of miR-21 antagomiR slowed the development of mechanical hypersensitivity (Figure 6C). If started 7 days after surgery, that is, after development of a full neuropathic phenotype, miR-21 antagomiR injections facilitated pain resolution after three injections (Figure 6D).

DISCUSSION

In this paper, we describe a novel role of miR-21 in both rodent neuropathic pain and patients with CRPS. MiR-21 impairs the BNB integrity in absence of trauma or inflammation and elicits neuropathic pain behavior. Furthermore, we provide a molecular pathway via inhibition of RECK, rise in MMP9 and, ultimately, claudin-1 downregulation. Linking our results to previous studies, we propose that miR-21 is a major switch in neuropathic pain: It affects pain behavior through different pathways, including inflammation-independent barrier impairment.

While miR-21 has been described in pain, research has mainly focused on its role in sensory DRG neuron–macrophage communication via exosomes[9] and on its proinflammatory effect, for example, stimulation of CC-chemokine ligand (CCL) 5 in nerves.[10] In addition, hypoxia and inflammatory mediators, such as cytokines, are major regulators of miR-21 transcription.[23,24] In our study, we observed miR-21 regulation in the peripheral nerve in both persistent neuropathic pain after permanent nerve transection (SNI) and transient neuropathy after nerve ligation (CCI). Alterations occurred independent of immediate nerve damage as the spared nerve was also affected. Moreover, miR-21 was also elevated in plasma of patients with CRPS (a human chronic pain syndrome with neuropathic features), supporting previous evidence (from a study using exosomes) with a much larger cohort and a more targeted control group.[5] While CCI models the neuropathic and neurogenic phenotype of CRPS,[25] SNI reflects the long duration. Thus, we identified miR-21 upregulation as an overarching feature, spanning neuropathic syndromes and species.

Application of miR-21 mimic to the intact nerve elicited strong mechanical hypersensitivity and a disruption of the BNB, similar to what is seen in SNI and CCI. The absence of nerval trauma or prior inflammation shows that miR-21 alone elicits the effects. In contrast,

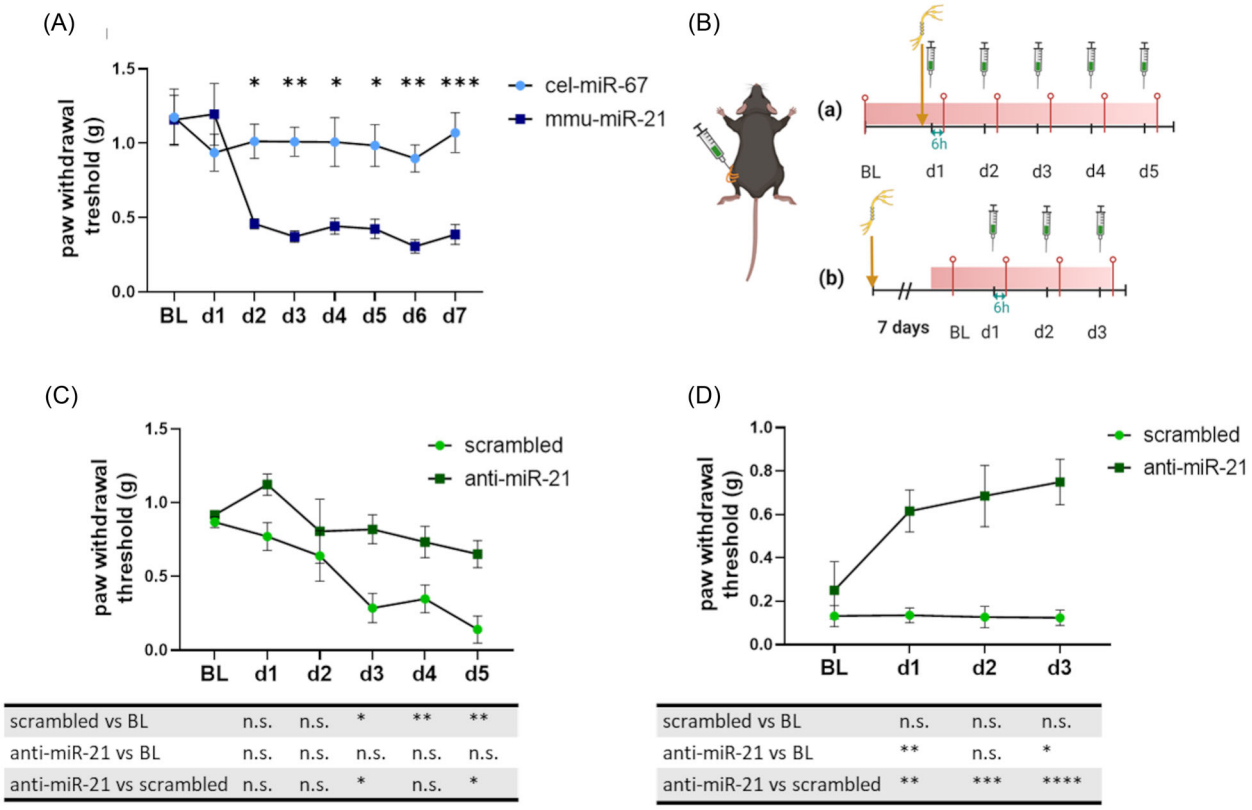

scrambled vs BL	n.s.	n.s.	*	**	**
anti-miR-21 vs BL	n.s.	n.s.	n.s.	n.s.	n.s.
anti-miR-21 vs scrambled	n.s.	n.s.	*	n.s.	*

scrambled vs BL	n.s.	n.s.	n.s.
anti-miR-21 vs BL	**	n.s.	*
anti-miR-21 vs scrambled	**	***	****

FIGURE 6 Mechanical hyperalgesia after perineural miR-21 mimic application and antinociception after antagomiR in CCI. (A) Paw withdrawal threshold after perineural injection of miR-21 mimic. $n = 8$, multiple unpaired *t*-tests with Holm–Sidak correction. (B) Injection scheme of antagomiR (a) starting directly after CCI, (b) starting 7 days after surgery. Injections were followed by behavioral testing with von Frey filaments after 6 h. Created with biorender®. (C, D) Paw withdrawal thresholds after perineural injection starting directly after CCI, C, or 7 days after surgery, D. $n = 8$. For comparison to BL: two-way ANOVA with Dunnett's multiple comparison test; for comparison between scrambled and antagomiR: one-way ANOVA with Sidak's multiple comparison test. $^{*}p < 0.05$, $^{**}p < 0.01$, $^{***}p < 0.001$, $^{****}p < 0.0001$. Abbreviation: BL, baseline

inhibition of miR-21 at the site of injury delayed and attenuated mechanical hypersensitivity. Our approach, studying antagomiR application both directly after surgery and after 7 days, demonstrated that miR-21 is essential for initiation, as well as maintenance, of neuropathic pain after nerve injury.

Characterizing miRNA targets and downstream cascades is rarely straightforward, as miRNAs can function pleiotropically. miR-21 is abundant in many tissues and cell types and highly conserved. Its many, often complementary, targets suggest that miR-21 functions as a master switch in many organ systems and diseases, for example, it plays a central role in homeostasis of the cardiovascular system.[26] In cancer, it can act both as an oncogene and tumor suppressor, depending on the cell type involved.[27] Moreover, miR-21 has been described as both anti- and proinflammatory.[28] Indeed, its proalgesic effect has previously been attributed to proinflammatory properties.[9,10] miR-21 plays a central role in nerve injury, both in cell–cell and intracellular communication. In hypoxic conditions, Schwann cell–derived miR-21 can promote neuron growth via PTEN.[29] On the other hand, miR-21 is central to Schwann cell differentiation and proliferation, development, as well as in peripheral nerve injury.[30,31]

In addition, the effects of miR-21 on barriers are variable. While miR-21-5p has a beneficial effect on endoneurial barriers, for example, the blood brain barrier after trauma,[32] the opposite has been described for miR-21-3p.[33] In contrast, in intestinal barrier breakdown, comparable to the perineurial rather than the endoneurial part of the BNB, miR-21-5p is increased.[34] The multifaceted roles of miRNAs become even more evident in heterocellular tissue, such as the nerve, which comprises not only axons and Schwann cells but also perineurial, endothelial, and immune cells. To focus on perineurial barrier effects, we used a claudin-1–dependent epithelial cell line (HT-29/B6), an established model for the perineurial barrier.[15,22] This allowed us to study the effect independent of possible influences from immune cells or cytokine release from other cell types.

In our study, we evaluated the effect of miR-21-5p on the BNB and particularly on claudin-1. As *in silico* analysis does not suggest a direct link between the two, we investigated possible pathways. miR-21 regulates the TGF-β signaling pathway by targeting mothers against decapentaplegic homolog 7 (SMAD7), ultimately leading to an increase in TGF-β.[35,36] In mice, nerve *Tgfb* is increased after nerve injury.[10] We explored *Tgfb* because it inhibits claudin-1 via MEK signaling.[16] In our study, *Tgfb* was increased in both animal models; however, in *vitro* testing did not show any effect of miR-21 incubation on *Tgfb*. Another known miR-21 target is RECK, which positively regulates claudin-1 via MMP9 inhibition.[15,37,36,38] We did observe regulation

of both RECK and MMP9 in murine nerve injury, as well as in a human epithelial cell line. The effect across species reflects the well-conserved sequence of miR-21 in mammals.[39] This translational aspect is crucial in recognizing the relevance of miR-21 in painful states. CRPS patients often suffer from edema, a symptom of barrier disruption, as well as trophic changes of hair, nails, and skin. Interestingly, MMP9 induces atrophy and is increased in the skin of CRPS-affected limbs.[40] Another miR-21 target and putative pathway gene *Pten* did not appear altered in the animal models we evaluated, and showed only late response to miR-21 incubation *in vitro* (data not shown). We do not attribute the hyperalgesic effect of miR-21—and the protective role of the antagomir—exclusively to its impact on the BNB. In concordance with a master switch function, we propose instead BNB disruption via RECK and MMP9 to be one independent factor that contributes to the overall proalgesic outcome.

Several miRNAs controlling BNB properties are regulated in pain. While barrier-impairing miR-155 is increased in CCI, possibly via tissue plasminogen receptor,[41] a reduction in miR-183 results in FOXO1-mediated claudin-5 reduction and subsequent endoneurial disruption.[42] CRPS patients show altered systemic levels of barrier-relevant miRNAs: both miR-183 and miR-223 are decreased in plasma-derived exosomes. Moreover, low miR-223 levels correlate with edema formation and a more severe clinical picture.[18] While exosomal miR-21 regulation has been described in CRPS,[5] its clinical significance is unclear.

Can miR-21 serve as a diagnostic or therapeutic tool in pain conditions? miR-21 is central to a variety of pathways and, consequently, is altered in different diseases. This lack of specificity impedes a possible role as biomarker.[43] However, miR-21 might be promising as a therapeutic target. In the last few years, miRNA-based treatment approaches have made great progress, with several techniques established to reduce immunogenicity, target-specific cell types, and allow different routes of administration.[44] Indeed, in the case of miR-21, local antagomiR application in mononeuropathy might be a viable option, comparable to approaches developed for other miRNAs.[45]

Our study has limitations. (1) Increased plasmatic miR-21 was independent of specific characteristics in CRPS like disease severity, duration, and (neuropathic) pain or trophic changes. (2) We did not measure downstream targets, such as MMP9 or RECK in CRPS patients; evaluation of a local effect requires skin biopsies, which we did not obtain in this study. Indeed, MMP9 expression is increased in the skin in CRPS.[40] Thus, this might be a promising pathway for future treatment. (3) Our *in vitro* analysis focused on an epithelial cell line; it is still not clear whether the perineurium is of epithelial or glial origin.[46] Also, we used a monoculture, while the nerve and its surroundings consist of very diverse tissues and cell types. Since we did observe a direct influence of miR-21 on these epithelial cells, this strengthens our claim of a direct regulation of the BNB, especially in the perineurium—while not excluding possible further pathways that might involve other cell types. (4) While our study focused on how miR-21 affects evoked mechanical hypersensitivity, further dimensions of neuropathic pain, including thermal hypersensitivity, spontaneous pain, and functional studies, including gait analysis, should be investigated in further projects.

In summary, we provide new evidence for the central role of miR-21 in neuropathic pain via regulation of the BNB. Local miR-21 targeting might be a promising treatment option in peripheral neuropathic pain and CRPS.

ACKNOWLEDGMENTS

We thank Bernhard Schwab and Joachim Schwabe for technical support and Andrea Prappacher for mouse husbandry. The project received financial support from IZKF Würzburg (Z-2/61), the EU 7FP grant "ncRNAPain" (Grant agreement 602133), and the German Research Foundation (DFG) (Clinical Research Unit KFO5001 "ResolvePAIN").

Open Access funding enabled and organized by Projekt DEAL.

COMPETING INTERESTS

The authors declare no competing interests.

AUTHOR CONTRIBUTIONS

A.K.R., F.K.S., M.M., C.S., and H.L.R. designed the study. A.K.R., S.M.K., E.S., and R.S.S. performed experiments. A.K.R., S.M.K., and H.L.R. analyzed data. All authors contributed to writing the manuscript.

ORCID

Susanne M. Krug https://orcid.org/0000-0002-1293-2484

REFERENCES

1. Birklein, F., Ajit, S. K., Goebel, A., Perez, R. S. G. M., & Sommer, C. (2018). Complex regional pain syndrome – Phenotypic characteristics and potential biomarkers. *Nature Reviews Neurology*, *14*, 272–284.
2. Reinhold, A. K., & Rittner, H. L. (2017). Barrier function in the peripheral and central nervous system-A review. *Pflugers Archiv: European Journal of Physiology*, *469*, 123–134.
3. Reinhold, A. K., Schwabe, J., Lux, T. J., Salvador, E., & Rittner, H. L. (2018). Quantitative and microstructural changes of the blood–nerve barrier in peripheral neuropathy. *Frontiers in Neuroscience*, *12*, 936.
4. Sauer, R. S., Krug, S. M., Hackel, D., Staat, C., Konasin, N., Yang, S., Niedermirtl, B., Bosten, J., Günther, R., Dabrowski, S., Doppler, K., Sommer, C., Blasig, I. E., Brack, A., & Rittner, H. L. (2014). Safety, efficacy, and molecular mechanism of claudin-1-specific peptides to enhance blood–nerve–barrier permeability. *Journal of Control Release*, *185*, 88–98.
5. Orlova, I. A., Alexander, G. M., Qureshi, R. A., Sacan, A., Graziano, A., Barrett, J. E., Schwartzman, R. J., & Ajit, S. K. (2011). MicroRNA modulation in complex regional pain syndrome. *Journal of Translational Medicine*, *9*, 195.
6. Kalpachidou, T., Kummer, K. K., & Kress, M. (2020). Non-coding RNAs in neuropathic pain. *Neuronal Signalling*, *4*, NS20190099.
7. Leinders, M., Üçeyler, N., Thomann, A., & Sommer, C. (2017). Aberrant microRNA expression in patients with painful peripheral neuropathies. *Journal of the Neurological Sciences*, *380*, 242–249.
8. Sakai, A., & Suzuki, H. (2013). Nerve injury-induced upregulation of miR-21 in the primary sensory neurons contributes to neuropathic pain in rats. *Biochemical and Biophysical Research Communications*, *435*, 176–181.
9. Simeoli, R., Montague, K., Jones, H. R., Castaldi, L., Chambers, D., Kelleher, J. H., Vacca, V., Pitcher, T., Grist, J., Al-Ahdal, H., Wong, L. F., Perretti, M., Lai, J., Mouritzen, P., Heppenstall, P., & Malcangio, M. (2017). Exosomal cargo including microRNA regulates sensory

neuron to macrophage communication after nerve trauma. *Nature Communication*, *8*, 1778.
10. Karl-Schöller, F., Kunz, M., Kreß, L., Held, M., Egenolf, N., Wiesner, A., Dandekar, T., Sommer, C., & Üçeyler, N. (2022). A translational study: Involvement of miR-21-5p in development and maintenance of neuropathic pain via immune-related targets CCL5 and YWHAE. *Experimental Neurology*, *347*, 113915.
11. Zhai, K., Duan, H., Wang, W., Zhao, S., Khan, G. J., Wang, M., Zhang, Y., Thakur, K., Fang, X., Wu, C., Xiao, J., & Wei, Z. (2021). Ginsenoside Rg1 ameliorates blood–brain barrier disruption and traumatic brain injury via attenuating macrophages derived exosomes miR-21 release. *Acta Pharmaceutica Sinica B*, *11*, 3493–3507.
12. Shi, C., Liang, Y., Yang, J., Xia, Y., Chen, H., Han, H., Yang, Y., Wu, W., Gao, R., & Qin, H. (2013). MicroRNA-21 knockout improve the survival rate in DSS induced fatal colitis through protecting against inflammation and tissue injury. *PLoS One*, *8*, e66814.
13. Wang, Y., Wang, S., & He, J. H. (2021). Transcriptomic analysis reveals essential microRNAs after peripheral nerve injury. *Neural Regeneration Research*, *16*, 1865–1870.
14. Kawasaki, Y., Xu, Z. Z., Wang, X., Park, J. Y., Zhuang, Z. Y. E., Tan, P. H., Gao, Y. J., Roy, K., Corfas, G., Lo, E. H., & Ji, R. U. R. (2008). Distinct roles of matrix metalloproteases in the early- and late-phase development of neuropathic pain. *Nature Medicine*, *14*, 331–336.
15. Hackel, D., Krug, S. M., Sauer, R. S., Mousa, S. A., Böcker, A., Pflücke, D., Wrede, E. J., Kistner, K., Hoffmann, T., Niedermirtl, B., Sommer, C., Bloch, L., Huber, O., Blasig, I. E., Amasheh, S., Reeh, P. W., Fromm, M., Brack, A., & Rittner, H. L. (2012). Transient opening of the perineurial barrier for analgesic drug delivery. *Proceedings of the National Academy of Sciences of the United States of America*, *109*, E2018–E2027.
16. Wang, K. E., Pascal, L. E., Li, F., Chen, W., Dhir, R., Balasubramani, G. K., Defranco, D. B., Yoshimura, N., He, D., & Wang, Z. (2020). Tight junction protein claudin-1 is downregulated by TGF-beta1 via MEK signaling in benign prostatic epithelial cells. *Prostate*, *80*, 1203–1215.
17. Kojima, T., Takano, K. I., Yamamoto, T., Murata, M., Son, S., Imamura, M., Yamaguchi, H., Osanai, M., Chiba, H., Himi, T., & Sawada, N. (2008). Transforming growth factor-beta induces epithelial to mesenchymal transition by down-regulation of claudin-1 expression and the fence function in adult rat hepatocytes. *Liver International*, *28*, 534–545.
18. Dietz, C., Müller, M., Reinhold, A. K., Karch, L., Schwab, B., Forer, L., Vlckova, E., Brede, E. M., Jakubietz, R., Üçeyler, N., Meffert, R., Bednarik, J., Kress, M., Sommer, C., Dimova, V., Birklein, F., & Rittner, H. L. (2019). What is normal trauma healing and what is complex regional pain syndrome I? An analysis of clinical and experimental biomarkers. *Pain*, *160*, 2278–2289.
19. Bennett, G. J., & Xie, Y.-K. (1988). A peripheral mononeuropathy in rat that produces disorders of pain sensation like those seen in man. *Pain*, *33*, 87–107.
20. Decosterd, I., & Woolf, C. J. (2000). Spared nerve injury: An animal model of persistent peripheral neuropathic pain. *Pain*, *87*, 149–158.
21. Dixon, W. J. (1965). The up-and-down method for small samples. *Journal of the American Statistical Association*, *60*, 967–978.
22. Yang, S., Krug, S. M., Heitmann, J., Hu, L., Reinhold, A. K., Sauer, S., Bosten, J., Sommer, C., Fromm, M., Brack, A., & Rittner, H. L. (2016). Analgesic drug delivery via recombinant tissue plasminogen activator and microRNA-183-triggered opening of the blood–nerve barrier. *Biomaterials*, *82*, 20–33.
23. Yang, C. H. E., Yue, J., Fan, M., & Pfeffer, L. M. (2010). IFN induces miR-21 through a signal transducer and activator of transcription 3-dependent pathway as a suppressive negative feedback on IFN-induced apoptosis. *Cancer Research*, *70*, 8108–8116.
24. Xu, X., Kriegel, A. J., Jiao, X., Liu, H., Bai, X., Olson, J., Liang, M., & Ding, X. (2014). miR-21 in ischemia/reperfusion injury: A double-edged sword? *Physiological Genomics*, *46*, 789–797.
25. Daemen, M., Kurvers, H., Kitslaar, P., Slaaf, D., Bullens, P., & Van Den Wildenberg, F. (1998). Neurogenic inflammation in an animal model of neuropathic pain. *Neurological Research*, *20*, 41–45.
26. Dai, B., Wang, F., Nie, X., Du, H., Zhao, Y., Yin, Z., Li, H., Fan, J., Wen, Z., Wang, D. W., & Chen, C. (2020). The cell type-specific functions of miR-21 in cardiovascular diseases. *Frontiers in Genetics*, *11*, 563166.
27. Pfeffer, S. R., Yang, C. H. E., & Pfeffer, L. M. (2015). The role of miR-21 in cancer. *Drug Development Research*, *76*, 270–277.
28. Sheedy, F. J. (2015). Turning 21: Induction of miR-21 as a key switch in the inflammatory response. *Frontiers in Immunology*, *6*, 19.
29. Cong, M., Shen, M. i., Wu, X., Li, Y., Wang, L., He, Q., Shi, H., & Ding, F. (2021). Improvement of sensory neuron growth and survival via negatively regulating PTEN by miR-21-5p-contained small extracellular vesicles from skin precursor-derived Schwann cells. *Stem Cell Research & Therapy*, *12*, 80.
30. Ni, Y., Zhang, K., Liu, X., Yang, T., Wang, B., Fu, L., & Yanmin Zhou, L. A. (2014). miR-21 promotes the differentiation of hair follicle-derived neural crest stem cells into Schwann cells. *Neural Regeneration Research*, *9*, 828–836.
31. Ning, X. J., Lu, X. H., Luo, J. C., Chen, C., Gao, Q., Li, Z. Y. U., & Wang, H. (2020). Molecular mechanism of microRNA-21 promoting Schwann cell proliferation and axon regeneration during injured nerve repair. *RNA Biology*, *17*, 1508–1519.
32. Ge, X., Huang, S., Gao, H., Han, Z., Chen, F., Zhang, S., Wang, Z., Kang, C., Jiang, R., Yue, S., Lei, P., & Zhang, J. (2016). miR-21-5p alleviates leakage of injured brain microvascular endothelial barrier *in vitro* through suppressing inflammation and apoptosis. *Brain Research*, *1650*, 31–40.
33. Ge, X., Li, W., Huang, S., Yin, Z., Yang, M., Han, Z., Han, Z., Chen, F., Wang, H., Lei, P., & Zhang, J. (2019). Increased miR-21-3p in injured brain microvascular endothelial cells after traumatic brain injury aggravates blood–brain barrier damage by promoting cellular apoptosis and inflammation through targeting MAT2B. *Journal of Neurotrauma*, *36*, 1291–1305.
34. Zhang, L., Zhang, F., He, D. K., Fan, X. M., & Shen, J. (2018). MicroRNA-21 is upregulated during intestinal barrier dysfunction induced by ischemia reperfusion. *Kaohsiung Journal of Medical Sciences*, *34*, 556–563.
35. Li, X., Yang, N., Cheng, Q. i., Zhang, H., Liu, F., & Shang, Y. (2021). MiR-21-5p in macrophage-derived exosomes targets Smad7 to promote epithelial mesenchymal transition of airway epithelial cells. *Journal of Asthma and Allergy*, *14*, 513–524.
36. Takahashi, C., Sheng, Z., Horan, T. P., Kitayama, H., Maki, M., Hitomi, K., Kitaura, Y., Takai, S., Sasahara, R. M., Horimoto, A., Ikawa, Y., Ratzkin, B. J., Arakawa, T., & Noda, M. (1998). Regulation of matrix metalloproteinase-9 and inhibition of tumor invasion by the membrane-anchored glycoprotein RECK. *Proceedings of the National Academy of Sciences of the United States of America*, *95*, 13221–13226.
37. Han, L., Yue, X., Zhou, X., Lan, F.-M., You, G., Zhang, W., Zhang, K.-L., Zhang, C.-Z., Cheng, J.-Q., Yu, S.-Z., Pu, P.-Y., Jiang, T., & Kang, C.-S. (2012). MicroRNA-21 expression is regulated by beta-catenin/STAT3 pathway and promotes glioma cell invasion by direct targeting RECK. *CNS Neuroscience & Therapeutics*, *18*, 573–583.
38. Wang, X., Miao, Y., Ni, J., Wang, Y., Qian, T., Yu, J., Liu, Q., Wang, P., & Yi, S. (2018). Peripheral nerve injury induces dynamic changes of tight junction components. *Frontiers in Physiology*, *9*, 1519.
39. Fromm, B., Domanska, D., Høye, E., Ovchinnikov, V., Kang, W., Aparicio-Puerta, E., Johansen, M., Flatmark, K., Mathelier, A., Hovig, E., Hackenberg, M., Friedländer, M. R., & Peterson, K. J. (2020). MirGeneDB 2.0: The metazoan microRNA complement. *Nucleic Acids Research*, *48*, D132–D141.
40. Escolano-Lozano, F., Gries, E., Schlereth, T., Dimova, V., Baka, P., Vlckova, E., König, S., & Birklein, F. (2021). Local and systemic expression pattern of MMP-2 and MMP-9 in complex regional pain syndrome. *Journal of Pain*, *22*, 1294–1302.

41. Reinhold, A. K., Yang, S., Chen, J. T. C., Hu, L., Sauer, R. S., Krug, S. M., Mambretti, E. M., Fromm, M., Brack, A., & Rittner, H. L. (2019). Tissue plasminogen activator and neuropathy open the blood–nerve barrier with upregulation of microRNA-155-5p in male rats. *Biochimica et Biophysica Acta - Molecular Basis of Disease*, *1865*, 1160–1169.
42. Reinhold, A. K., Salvador, E., Förster, C. Y., Birklein, F., & Rittner, H. L. (2021). Microvascular barrier protection by microRNA-183 via FoxO1 repression: A pathway disturbed in neuropathy and complex regional pain syndrome. *Journal of Pain*.
43. Jenike, A. E., & Halushka, M. K. (2021). miR-21: A non-specific biomarker of all maladies. *Biomarker Research*, *9*, 18.
44. Winkle, M., El-Daly, S. M., Fabbri, M., & Calin, G. A. (2021). Noncoding RNA therapeutics — Challenges and potential solutions. *Nature Reviews Drug Discovery*, *20*, 629–651.
45. Van Der Ree, M. H., De Vree, J. M., Stelma, F., Willemse, S., Van Der Valk, M., Rietdijk, S., Molenkamp, R., Schinkel, J., Van Nuenen, Ad. C., Beuers, U., Hadi, S., Harbers, M., Van Der Veer, E., Liu, K., Grundy, J., Patick, A. K., Pavlicek, A., Blem, J., Huang, M., … Reesink, H. W. (2017). Safety, tolerability, and antiviral effect of RG-101 in patients with chronic hepatitis C: A phase 1B, double-blind, randomised controlled trial. *Lancet*, *389*, 709–717.
46. Kucenas, S., Takada, N., Park, H. C., Woodruff, E., Broadie, K., & Appel, B. (2008). CNS-derived glia ensheath peripheral nerves and mediate motor root development. *Nature Neuroscience*, *11*, 143–151.
47. Kreusel, K. M., Fromm, M., Schulzke, J. D., & Hegel, U. (1991). Cl-secretion in epithelial monolayers of mucus-forming human colon cells (HT-29/B6). *American Journal of Physiology*, *261*, C574–C582.
48. Li, H., Zhao, J., Jia, X., Zhang, Y., Du, Y., Li, H., Ma, L., & Huang, J. (2020). miR-21 promotes growth, invasion and migration of lung cancer cells by AKT/P-AKT/cleaved-caspase 3/MMP-2/MMP-9 signaling pathway. *International Journal of Clinical and Experimental Pathology*, *13*, 692–700.
49. Li, Q., Li, B., Li, Q., Wei, S., He, Z., Huang, X., Wang, L., Xia, Y., Xu, Z., Li, Z., Wang, W., Yang, L., Zhang, D., & Xu, Z. (2018). Exosomal miR-21-5p derived from gastric cancer promotes peritoneal metastasis via mesothelial-to-mesenchymal transition. *Cell Death & Disease*, *9*, 854.

SUPPORTING INFORMATION

Additional supporting information can be found online in the Supporting Information section at the end of this article.

How to cite this article: Reinhold, A. K., Krug, S. M., Salvador, E., Sauer, R. S., Karl-Schöller, F., Malcangio, M., Sommer, C., & Rittner, H. L. (2022). MicroRNA-21-5p functions via RECK/MMP9 as a proalgesic regulator of the blood nerve barrier in nerve injury. *Ann NY Acad Sci*., *1515*, 184–195. https://doi.org/10.1111/nyas.14816